AUT Journal of Civil Engineering

AUT J. Civil Eng., 6(1) (2022) 3-14
DOI: 10.22060/ajce.2022.19547.5740

Reliability of Single-Layer Steel Space Domes under the Effects of the Changes in the Height-to-Span Ratio

A. Bahrpeymah[1]*, M. Layegh Rafat[2], N. Shabakhty[3]

[1] Department of Civil Engineering, University of Sistan and Baluchestan, Zahedan, Iran.
[2] Department of Civil Engineering, Zabol Branch, Islamic Azad University, Zabol, Iran.
[3] School of Civil Engineering, Iran University of Science and Technology, Tehran, Iran.

ABSTRACT: In space domes, geometrical changes are the main factors that determine the forces in the structural members. This paper has addressed the effects of the height-to-span ratio variations on the reliability of space domes. Applied loads, nodes coordinates, member's cross-section, modulus of elasticity, and yield stress are the random variables, and FORM (first-order reliability method), SORM (second-order reliability method), MCS (Monte Carlo sampling) and IS (importance sampling) were the methods used to evaluate the reliability of such structures. Results showed that FORM yielded better solutions; reliability increased with an increase in the height-to-span ratio, and a change in the performance function changed the reliability index and sensitivity coefficient. Hence, for domes with height-to-span ratios less than 0.3, the displacement performance function is the effective function and for ratios greater than 0.3, the stress performance function should be considered as the critical function.

Review History:

Received: Jan. 24, 2021
Revised: Jul. 29, 2022
Accepted: Sep. 03, 2022
Available Online: Sep. 11. 2022

Keywords:

Reliability index
Sensitivity
Correlation
Performance function
Height-to-span ratio

1- Introduction

In space structures, since external loads, internal forces and displacements do not lie in one plane, all three dimensions affect the structure's behavior [1]. In general, these structures are grouped as grids, drums, and domes [2], but the latter is more popular because, compared to other structural forms, they are beautiful, light, and economical, behave properly against applied loads, and are very popular, especially where mid pillars are not desirable [3]. Depending on their span length, space domes are either single- or double-layered (the latter are used in larger spans [4]), and since they often have higher degrees of uncertainty, they are expected to be highly safe against failure. However, recent evidence shows that, in different parts of the world, some of them have failed or fractured under snow/wind/earthquake loads, or because of traditional designs that neglect uncertainties in materials and applied loads [5]. As the behavior of a space structure, with hundreds or even thousands of members and nodes, depends on some uncertainties or random parameters, its reactions, too, have a random nature and it is necessary to consider the uncertainties of the system parameters in evaluating its actual behavior [6]. Among a limited number of research on the safety and reliability of space structures, most have addressed their optimization, buckling characteristics, failure mechanisms, and seismic behavior. Li Hui *et al.* [7] studied the reliability, sensitivity, and correlation among the random variables in tree structures (a special space structure). Kubicka *et al.* [8] studied flat space structures considering the effects of the temperature rise and the node-connection type on the reliability. Tahamouli *et al.* [9] studied space structures with different supports considering the effects of the defects of random members on the reliability. In recent years, some researchers have studied the reliability of large-span space structures (double-layered domes and grid drums) [10-11]. If the height-to-span ratio (an important design parameter) varies in a space dome, the loading and, hence, the forces will also change in the members, meaning that geometry and its changes are the main factors in determining the forces created in the members of the dome, i.e. the structure weight is directly related to the height-to-span ratio. Since these structures are designed and constructed on large scales, determining the most suitable height-to-span ratio to achieve the minimum weight is quite important. Yang *et al.* [12] optimized the height of a 120-member dome as a design variable, Salajegheh *et al.* [13] optimized the geometry (found minimum weight) of single-layered space domes with fixed spans and heights considering the meridian equation power and orbit radius as the design variables, Saka [14] used the GA to optimize a geodesic dome considering the crown height and member cross-section as random variables. Hasacebi *et al.* [15] proposed an algorithm to optimize the topology of geodesic domes. Shao Qi *et al.* [16] analyzed the

*Corresponding author's email: bahrpeyma@usb.ac.ir

uncertainty and parametric sensitivity of lattice space domes under blast loading and showed that the structure response to blast parameters was very sensitive. Zhou *et al.* [17] evaluated the resistance against the progressive collapse of the Zhongchuan Airport Terminal Building in China, which is a large-span curved space structure, and showed that the structure had enough supporting load transfer path that could effectively prevent the progressive collapse after the initial failure. Jahangir *et al.* [18] used the multiple nonlinear regression approach to investigate the cyclic behavior of steel-bar hysteretic dampers. Farhangi *et al.* [19] used machine learning techniques to study the behavior of steel-bar hysteretic dampers equipped with shape memory alloy. Pakseresht and Gholizadeh [20] addressed the size-topology optimization and reliability evaluation of three types of single-layered lattice space domes and showed, as their most important finding, that the reliability indices of most optimally designed domes were low; hence, they were not safe against total collapse. Tian *et al.* [21] studied the resistant performance against the collapse of long-span, single-layered, lattice, space structures subjected to concentrated impact loads and showed that their dynamic performance was significantly affected by the duration of the applied impact load. Zhang *et al.* [22] presented a new method to estimate the dynamic failure of single-layer mesh domes' underground acceleration according to the response spectrum of the China earthquake.

Since a literature review showed that past research neglected to study the space dome geometry effects on reliability, this paper evaluated the reliability of steel, single-layered space domes under different height-to-span ratios to examine the sensitivity and correlation among their random variables under dead and snow loads using two performance functions: 1) maximum displacement in nodes and 2) maximum stress in members for reliability analyses and four methods (FORM, SORM, MCS, and IS) for reliability index evaluations considering the elasticity modulus, yield stress, applied loads, nodes coordinates and members cross sections as random variables.

2- Performance functions

Performance or limit state function shows the structural safety-failure boundary mathematically as follows:

$$g(R,S)=R-S \tag{1}$$

Where R and S are the load and strength random variables, respectively, and g divides the space into R_s and R_f (safe and failure regions); failure occurs when g (limit state function) < 0.

$$g(X)=\begin{cases}>0, X\in R_s\\ \le 0, X\in R_f\end{cases} \tag{2}$$

Hence, from a structural point of view, when a structure response exceeds its corresponding strength, the system will fail [23]. This paper has considered two failure modes to define the performance function: when allowable limits (given in the Code) are violated by 1) a member maximum stress and 2) a node maximum displacement.

2- 1- Displacement performance function

Shown below, this function shows the deformation limits of the nodes of a dome structure:

$$g_{idispl}=1-\frac{\left|\delta_i(X)\right|}{\delta_a} \qquad i=1,2\cdots n \tag{3}$$

Where $\delta_i(X)$ is the displacement of node i, n is the total number of nodes, δ_a is the allowable node displacement with a maximum value limited to $\delta_H=H/300$ in the horizontal direction and $\delta_V=D/360$ in the vertical direction, and D and H are the dome diameter and height, respectively [24].

2- 2- Stress performance function

When single-layered space domes are exposed to external loads, the internal forces created in their members are mainly axial tension and compression; in tension, the governing criterion is yielding and in compression, it is buckling. The limit state function is as follows:

$$g_{istress}=1-\frac{\left|\sigma_i(X)\right|}{\sigma_a} \qquad i=1,2\cdots,m \tag{4}$$

$$\sigma_a=\min\left(\sigma_{cr},\sigma_y\right) \tag{5}$$

Where σ_i is the tension among the i^{th} member and σ_a is the maximum allowable stress found based on the AISC-ASD Code [25]. Under tension, the member's allowable tensile stress is as follows:

$$\sigma_y=F_y \tag{6}$$

And under compression, its allowable compressive stress is found as follows:

A) For inelastic buckling $\lambda_i<C_c$:

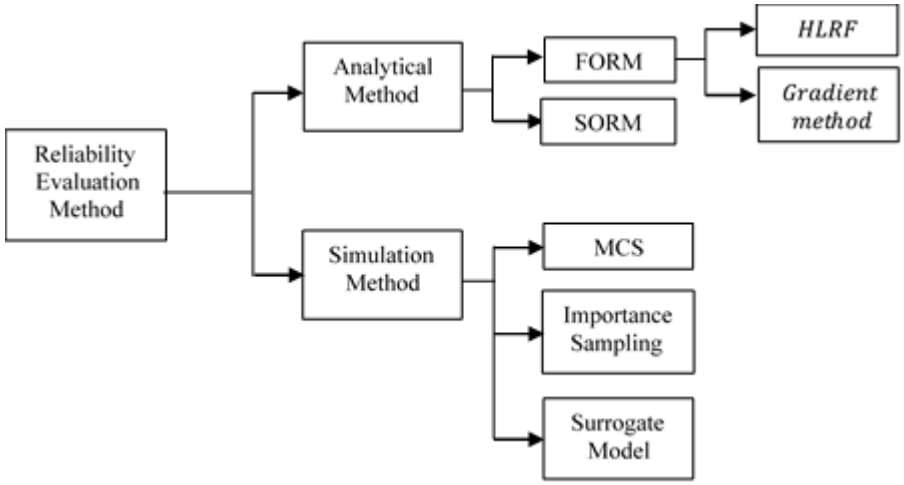

Fig. 1. Classification of reliability evaluation methods [30].

$$\sigma_{cr} = \left(1 - \frac{\lambda_i^2}{2C_c^2}\right) \times F_y \tag{7}$$

B) For elastic buckling ($\lambda_i \geq C_c$):

$$\sigma_{cr} = \left(\frac{\pi^2 E}{\lambda_i^2}\right) \tag{8}$$

where E is the elasticity modulus, F_y is the steel yield stress, $\lambda_i = \frac{KL_i}{r_i}$ is the member slenderness coefficient, L_i and r_i are respectively the length and radius of gyration of the i^{th} member, FS is the factor of safety (= 1 in all above relations in the reliability analyses), C_c is the critical slenderness (showing if the member is slender, medium, or fat), and k_i is the i^{th} member's effective length coefficient (= 1 in the present study). The AISC has limited the maximum slenderness coefficient to 300 for members under tension and 200 for those under compression [25]. Considering the limit state function given in Eq. (2), P_f (failure probability) can be obtained as follows:

$$P_f = P(g(X) \leq 0) = \int_{g(X)\leq 0}^{0} f_X(x)dx \tag{9}$$

Where $f_X(x)$ the random variables' joint probability density is function and P_f is the volume under the surface of $f_X(x)$ in the $g(X) \leq 0$ failure region [26]. Since $f_X(x)$ is complex, especially for variables with non-normal distributions, its analytical solution will not yield P_f and its time-consuming numerical solution is possible only for a few random variables. Therefore, in most cases, P_f is found by such approximate reliability index-based methods as the FORM and SORM or by such simulation-based methods as MCS and IS [27, 28, and 29]. Classification of the reliability evaluation methods is shown in Fig. 1.

3- Simulation methods

Simulation is an effective and accurate method used to assess the reliability of structures with complex limit state functions where other methods fail to estimate P_f . In general, P_f is found based on the reliability analysis as follows:

$$P_f = \int_{g(X)\leq 0}^{0} f_X(x)dx \tag{10}$$

where $f_x(x)$ is the variables' joint probability density function, $g(X)$ is the failure zone found by one or more limit state functions and X is a random variable Eq. (11) that can be used to find P_f by the MCS method for each failure mode (*N* sample points based on f_X):

$$P_f = \frac{1}{N}\sum_{i=1}^{N} I(g(x_i) < 0) f_X(x_i) \tag{11}$$

Where N is the number of sample points and I is the counter function ($\mathrm{I}(0) = 1$ for samples in the failure zone and $\mathrm{I}(0) = 0$ in other zones). In this method, high precision requires many samples which are produced with high computational costs, especially when P_f is small or the structure is large-scale. These costs are reduced using pseudo MCS methods [31] such as the IS where a simulation variable

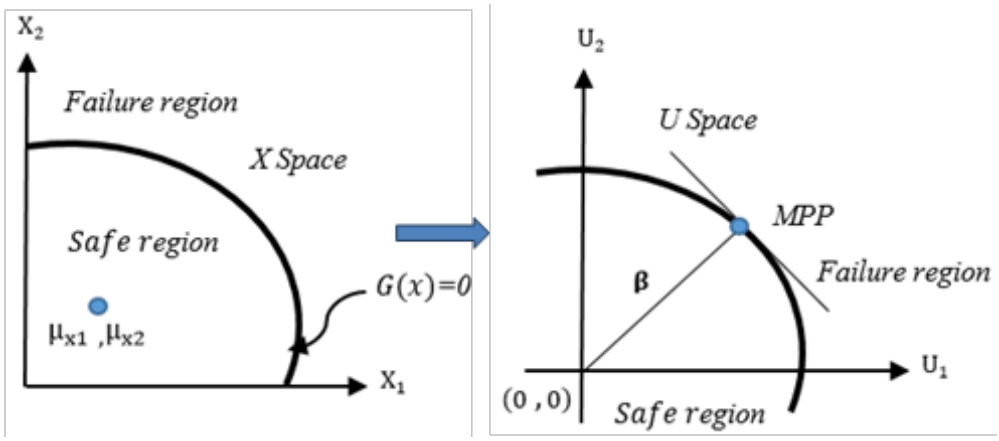

Fig. 2. Transforming X-space to U-space [34].

V is selected with a new probability density function $h_V(V)$ (called "IS density function") that generates the maximum samples in zones that highly affect the structural failure in space X; P_f is found as follows:

$$P_f = \int_D \cdots \int \left\{ I(V) \frac{f_x(V)}{h_V(V)} \right\} h_V(V) dx \tag{12}$$

$$P_f = \frac{1}{N} \sum_{i=1}^{n} \left(I(V_i) \frac{f_x(V_i)}{h_V(V_i)} \right) \tag{13}$$

Where $I(V)$ is a marker function (= 1 for points in the failure zone and = 0, otherwise) [32].

4- Analytical reliability method

Calculating P_f requires multiple integrations of Eq. (9), which is a very difficult task; hence, common numerical estimation methods such as FORM and SORM are used to simplify the process. FORM, proposed in 1974 by Hasofer Lind [33]. Calculating the reliability is a very widely used method where the reliability index does not change for various forms of a specified limit state function under similar random variables' mapping [34]. In this method, random variables are transferred from the design space to the normal standard space (Mean=0, Standard deviation=1) and provide a new reliability index as the minimum geometric distance between the origin and the transferred limit state function. Hasofer Lind [33] defined the design point as the point on the limit state function $(g = 0)$ with the shortest distance from the origin in the normal standard space. This point is referred to as the maximum probability point (MPP) (Fig. 2) and its distance from the origin is the reliability index (P_f is found from $p_f = \phi(-\beta)$). Hence, the design point can be found by the following optimization algorithm:

$$\begin{aligned} &\text{Minimize} \quad \beta = \sqrt{\sum_{i=1}^{n} U_i^2} \\ &\text{Subject to} \quad g(U) = 0 \end{aligned} \tag{14}$$

Where U_i is the i^{th} random variable in the standard normal space and n is the number of random variables. General optimization methods or point search algorithms with the highest P_f presented by Hasofer Lind -Rackwitz Fiessler (HLRF) and the gradient method (specific to FORM) can be used to solve Eq. (14).

4- 1- Hasofer Lind - Rackwitz Fiessler (HLRF) method

The optimization model in Eq. (14) can be solved by the Hasofer Lind-Rackwitz Fiessler (HLRF) method [35] that uses an iterative search method as follows to find the minimum distance:

$$U_{m+1} = U_m + s_m d_m \tag{15}$$

Where m is the number of iterations, s_m is the step length and d_m is the search direction vector found from the following relation:

$$d_m = \frac{\nabla^T g(U_m) U_m - g(U_m)}{\nabla^T g(U_m) \nabla g(U_m)} \nabla g(U_m) - U_m \tag{16}$$

Where $\nabla g\left(U_m\right)$ is the vector of the limit state function derivative at point U_m Substituting Eq. (16) in Eq. (15) to solve the optimization problem, the Hasofer Lind-based reliability equation will be as follows:

$$U_m^{HL}=\frac{\nabla^T g\left(U_m\right)U_m-g\left(U_m\right)}{\nabla^T g\left(U_m\right)\nabla g\left(U_m\right)}\nabla g\left(U_m\right) \tag{17}$$

In this method, a point in the possible region moves towards a point with the maximum MPP on the limit state function [34].

4- 2- Gradient method

To find the reliability index, the gradient method uses the iterative search method of Eq. (15) where the search direction vector (d_m) is so determined at the desired surface (based on the objective function) that the problem may, in each iteration, lie in the allowable range; hence, it should satisfy the limit state function $g\left(U_m\right)=0$ and its gradient $\nabla g\left(U_m\right)=0$. The new search direction vector is then expressed as follows:

$$d_m=\frac{\nabla^T g\left(U_m\right)U_m}{\nabla^T g\left(U_m\right)\nabla g\left(U_m\right)}\nabla g\left(U_m\right)-U_m \tag{18}$$

When the problem constraints are nonlinear, the new point obtained by Eq. (15) cannot satisfy the limit states as a constraint; therefore, the Newton iterative algorithm (Eq. (19)) is used to push the new point on the failure surface in the standard normal space.

$$U_{m+1}^{i+1}=U_{m+1}^{i}+\frac{g\left(U_{m+1}^{i}\right)}{\left\|\nabla g\left(U_{m+1}\right)\right\|^2}\nabla g\left(U_{m+1}\right) \tag{19}$$

The gradient method uses the information of the first derivative of the reliability function (Eq. (14)), and since it has an equality constraint, it can be used for any reliability problem [36]. The first-order reliability algorithm is usually suitable for limit state functions near linear design points, but when the fracture surface has a large curvature, this algorithm cannot estimate the safety index effectively and accurately. Hence, a second-order curvature surface is used in the second-order reliability method to approximate the limit state function at the design point. When the curvature of a curved surface conforms to that of the limit state function, the failure probability in the second-order approximation method is found as follows:

$$p_f=P\left\{g(X)\le 0\right\}=\Phi(-\beta)\prod_{i+1}^{n-1}(1+\beta k_i)^{\frac{1}{2}} \tag{20}$$

Where k is the limit state function curvature at MPP and n is the No. of random variables [37].

5- Reliability-based sensitivity analyses

In this method, the reliability index sensitivity is found through a small turmoil in the random variables. First-order estimation methods present the importance factor $\left(\alpha_i^2\right)$ as a function of the linearized limit state function derivative. These factors are the conductor cosines vector in the search process that should satisfy the following relation:

$$\alpha_1^2+\alpha_2^2+\cdots+\alpha_i^2=1 \tag{21}$$

Where α_i is, in fact, the sensitivity coefficient of the reliability index at the point with the highest P_f and its physical meaning shows the relative share of each random variable from P_f (the variable with the highest sensitivity coefficient that has the greatest share in determining the problem reliability index). Using the definition of the reliability index (β), which is the distance of the limit state function at point0 = $g\left(U\right)$ from the origin in the normal standard space [36], we will have:

$$\frac{\partial\beta}{\partial u_i}=\frac{\partial}{\partial u_i}\left(\sqrt{u_1^2+u_2^2+\cdots+u_i^2}\right)=\frac{u_i}{\beta}=\alpha_i \tag{22}$$

6- Coefficient of correlation among random variables

Correlation can be defined as the effects of a random variable on other variables or the degree of linear dependence between two variables; hence, the linear correlation is best defined by a coefficient as follows:

$$\rho_{XY}=\frac{\operatorname{cov}\left[X,Y\right]}{\sqrt{\operatorname{var}\left[X\right]\operatorname{var}\left[Y\right]}} \tag{23}$$

Where ρ_{XY} is the correlation coefficient between random variables X and Y with averages μ_x and μ_y and standard deviations σ_x and σ_y and $COV\left[X\,Y\right]$ is the covariance between them defined as follows:

$$\operatorname{cov}\left[X,Y\right]=E\left[\left(X-\mu_x\right)\left(Y-\mu_y\right)\right] \tag{24}$$

Since ρ_{XY} is an important parameter in structure safety calculations ($-1\le\rho\le 1$), ρ_{XY} = 0 means that variables are independent (lack correlation) and its positive and negative values mean direct and inverse relations, respectively [23].

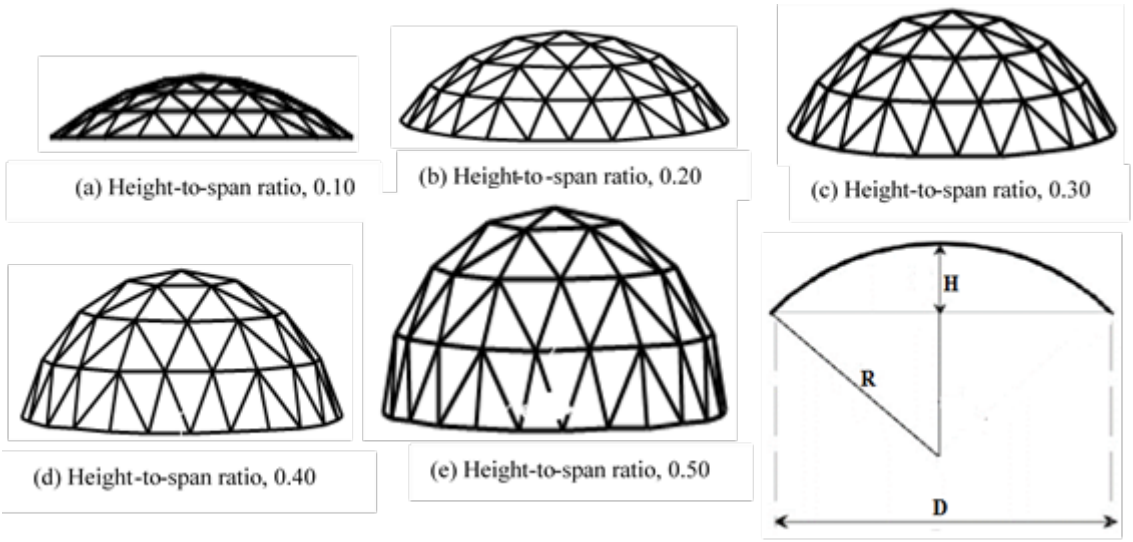

Fig. 3. Side view of a space dome with five different height-to-span ratios.

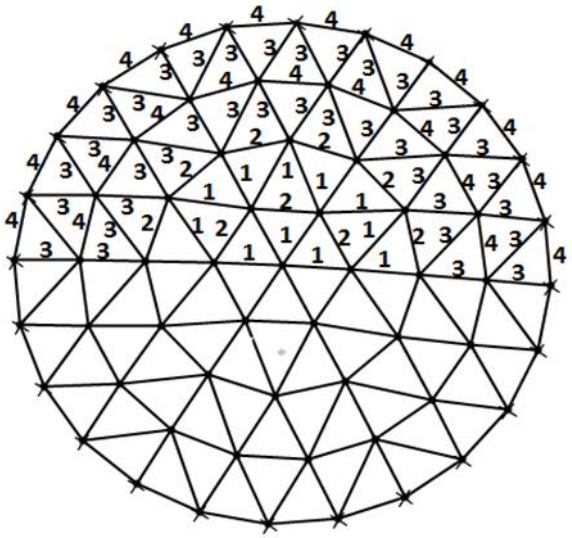

Fig. 4. Dome-space member groups.

7- Finding the reliability of single-layered space domes by the height-to-span ratio

7- 1- Model description and random parameters

This section examines five dome structures with height-to-span ratios of 0.1, 0.2, 0.3, 0.4, and 0.5 (Fig. 3) each having 156 hollow-steel-pipe members divided into 4 groups (Fig. 4), 61 nodes and 20m span length with curvature radii of 26, 14.50, 11.33, 10.25, and 10 m, respectively. The domes have been designed under 3 different load combinations as follows: The equipment load, which is concentrated and usually acts on the structure vertex vertically, is $10\,kN$, and the dead load, including the weights of the members, joints, structure cover, and snow, is $0.2\,kN/m^2$. These loads were calculated, assuming a covered structure surface (nodes' effective loading surface), to find unequal concentrated forces acting on the nodes. Elasticity modulus, yield stress, dead and snow loads, nodes' coordinates in the Z-direction, and section-area of members were random variables, and their statistical characteristics including the probability distribution type, mean and standard deviation are listed in Table 1.

Table 1. Statistical parameters of random variables.

R. V.	Description	Distribution	mean	COV
P_d(kN)	Dead load	Gauss	1.03	5%
P_s(kN)	Snow load	Gauss	7.13	30%
E(kN/cm^2)	Young s modulus	Lognormal	2.059e4	5%
F_y(kN/cm^2)	Yield strength	Lognormal	23.536	5%
A_1(cm^2)	Cross-sectional area	Lognormal	9.50	5%
A_2(cm^2)	Cross-sectional area	Lognormal	6	5%
A_3(cm^2)	Cross-sectional area	Lognormal	8	5%
A_4(cm^2)	Cross-sectional area	Lognormal	5.5	5%
Z_i(cm)	Nodal coordinates in z directions	normal	---	3cm

Table 2. Reliability indices, consumed time, and errors of several reliability methods.

	FORM		SORM	IS	MCS(1000000)
	HLRF	Gradient method			
β	2.528	2.527	2.543	2.552	**2.570**
Time (s)	12	8	28	1285	**15425**
Error	1.65%	1.64%	1.06%	0.705%	**.....**

Table 3. Comparing the effects of different performance functions on the reliability index for different height-to-span ratios.

H/D	0.10	0.20	0.30	0.40	0.50
$\beta_{Displacement}$	1.450	2.527	4.880	12.428	**16.492**
β_{Strsse}	2.211	3.135	4.372	4.896	**6.363**

7- 2- Efficiency and accuracy of different reliability methods

In space structures, random variables are numerous and the reliability index determination is quite time-consuming. Hence, this section tries to propose a method that can find this index quickly and precisely using FORM, SORM, IS, and MCS for the required analyses and the vertical displacement performance function for the vertex node because it has the highest displacement; the allowable vertical displacement is assumed to be 2.5 cm. Accordingly, space dome *b* with a height-to-span ratio of 0.2, and geometric and statistical specifications given in Table 1 was selected for reliability analyses with an Intel (R) Core i5 CPU M480 @ 2.67GHz computer and the results are shown in Table 2. As shown, FORM, the fastest among the presented methods, has used both the Hasofer Lind and Gradient algorithms to calculate the reliability index. Although the two values are not significantly different, the convergence speed of the gradient-based FORM is greater than that of the Hasofer Lind method. If the MC-based calculated reliability index is assumed as a reference, the relative error of the gradient-based FORM is 1.65% compared to the reference. SORM requires 28 sec to calculate the reliability index and the error in this method is about 1.06% which is less than that of the FORM. The IS error is less than those of FORM and SORM, but its calculation time is 1285 sec; the slowest is MCS with 15425 sec. It can be concluded, in general, that in space structures with numerous random variables, simulation methods are not cost-effective because they are quite time-consuming.

Therefore, FORM and SORM (approximation methods) are preferable for reliability index calculations. SORM yields better results than FORM because it uses a parabolic surface to approximate the limit state function; however, its calculation time increases significantly with an increase in the number of random variables because it requires a second-order derivative. A comparison of the two methods can reveal that their reliability indices are close and FORM can be used to continue the work.

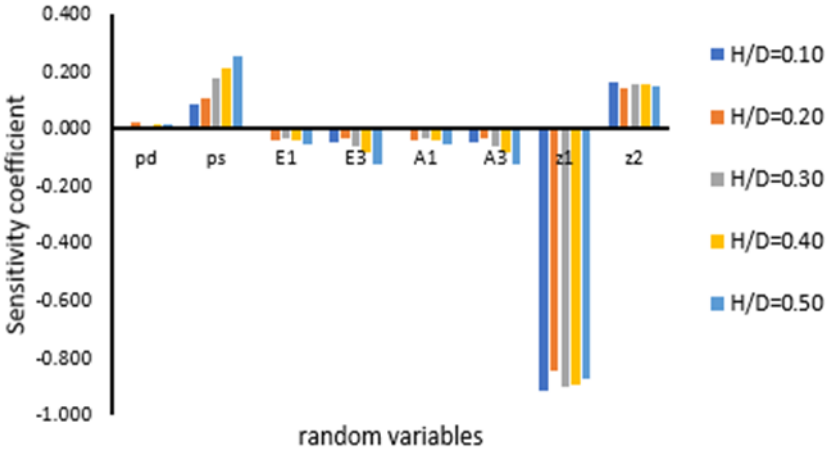

Fig. 5. Sensitivity coefficient of the displacement limit state function g1 vs. random variables.

7- 3- Comparing the effects of different performance functions on finding the reliability Index

Past studies have generally used the displacement performance function to assess the reliability of space structures, but this paper has used different height-to-span ratios to study the effects of the displacement and stress performance functions (g_1 and g_2) on determining the reliability index; results from the FORM reliability analyses are given in Table 3. As shown, an increase in the height-to-span ratio increases the reliability index because the former will change the loading and arch behavior of the dome structures. For both the displacement and stress performance functions, the minimum reliability index is related to a height-to-span ratio of 0.1.

In this case, the domes are relatively flat and shallow, and the internal forces created in the members (by external loads) are mainly bending moments that create small axial forces in the members. Here, the dome behavior resembles that of a flat**,** single-layered, grid system that has small stiffness and large deformations under external loads perpendicular to the structure plane.

An increase in the height-to-span ratio reduces the effects of the external loads (snow) and arch behavior of the structure creating axial forces in the members and reducing their bending moments, causing them to deform. At a height-to-span ratio of 0.50, the arch behavior increases the structural stiffness and highly reduces its displacement. It means that an increase in the height-to-span ratio increases the structure bearing capacity and, hence, increases the reliability. Therefore, in domes with a height-to-span ratio < 0.3, g_1 is the suitable displacement performance function and for ratios > 0.3, g_2 (the stress performance function) should be considered as the effective (critical) limit state function. In short, it can be concluded that a change in the height-to-span ratio in space domes changes the structure's performance function.

7- 4- Sensitivity analyses of space domes with different height-to-span ratios

This section has done the sensitivity analyses of the displacement and stress performance functions (g_1 and g_2) for random variables of domes with height-to-span ratios of 0.1, 0.2, 0.3, 0.4, and 0.5 (Figs. 5 and 6) considering the member cross-section, elasticity modulus, yield stress, snow and dead loads and nodes' coordinates (in the vertical direction) as random variables. Since the applied load and structure shape are symmetrical, the sensitivity coefficient is the same for nodes located in each ring. Hence, one node is selected from each ring because the space is not enough; z_1 is node 1 (vertex), z_2 is the node in ring 1, z_7 is the node in ring 2, and z_{19} is the node in ring 3. Some random parameters have been neglected because of their small sensitivity coefficients and negligible effects. According to Figs. 5 and 6, an increase in the height-to-span ratio gradually increases the sensitivity of the coefficients of the displacement and stress performance functions to the changes in the external loads. Since an increase in the height-to-span ratio reduces the maximum deformation in these domes, the increase in the sensitivity coefficient of the displacement performance function would be less than that of the stress performance function.

7- 5- Inter-random variable correlation effects on the reliability

Since it is rather rare, in engineering problems, that effective parameters of a structure may not correlate, it is necessary to consider the correlation coefficient to arrive at real and more accurate solutions. This section has studied the effects of the variations of this coefficient on the reliability, for materials and geometry of space domes with different height-to-span ratios, considering the elasticity modulus and yield stress of the members and assuming other random variables to be independent (Table 4).

Table 4. Effects of correlation coefficient variations on the reliability index.

	ρ_{EF_y}	-1.0	-0.80	-0.40	0.00	0.40	0.80	1.00
β	h/D 0.10	2.1937	2.1929	2.1913	2.1897	2.1881	2.1864	**2.1856**
	0.20	3.1369	3.1364	3.1352	3.1347	3.1343	3.1337	**3.1335**
	0.30	4.3721	4.3721	4.3721	4.3721	4.3721	4.3721	**4.3721**
	0.40	4.8963	4.8963	4.8963	4.8963	4.8963	4.8963	**4.8963**
	0.50	6.3641	6.3641	6.3641	6.3641	6.3641	6.3641	**6.3641**

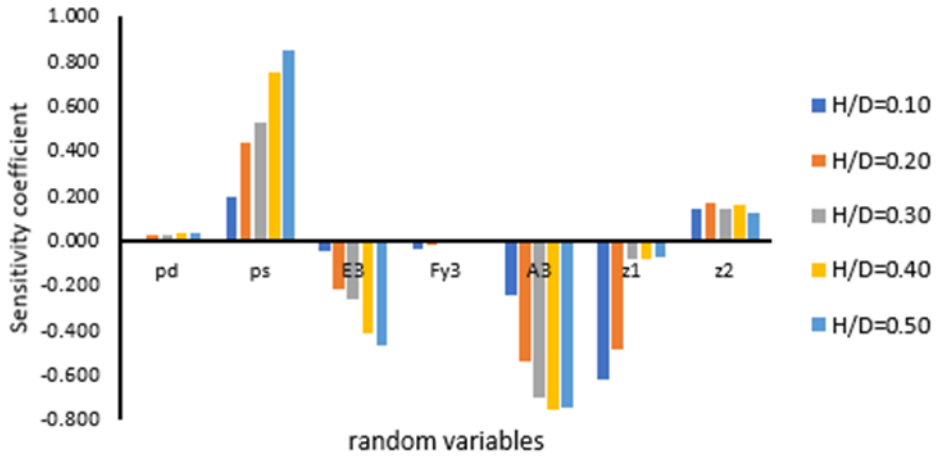

Fig. 6. Sensitivity coefficient of the stress limit state function g2 vs. random variables.

As shown, for space domes with height-to-span ratios of 0.1 and 0.2, failure occurs due to yield stress (which is related to the elasticity modulus) because the members' high bending moments and low slenderness cause the stress to exceed the yield point in some members; hence, a change in the correlation coefficient ρ_{EF_y} changes the reliability. However, for 0.3, 0.4, and 0.5 ratios, the mentioned change has no effects on the reliability because the axial stress is high at these ratios and the bending is negligible, which means axial behavior is dominant in the members. On the other hand, an increase in slenderness causes the maximum stress to occur due to buckling (buckling stress is found in Euler's formula). Therefore, buckling stress is dependent on the elasticity modulus rather than on the yield stress. Next, to study the inter-node correlation effects on the reliability of space domes, one node is selected from each ring. Here, the nodes are z_1, z_2, z_7, and z_{19}, and the reliability is calculated by changing the coefficient of correlation between every two nodes assuming it to be zero for other nodes. According to Fig. 7, the correlation coefficient variation between z_1 and z_2 ($\rho_{Z_{1Z_2}}$) has the greatest effect on reliability. For positive correlation coefficients, an increase in the coefficient will increase the reliability, but for negative ones, the increase will reduce it; in other nodes, this variation does not affect the reliability considerably. Fig. 8 shows the correlation coefficient variations between nodes z_1 and z_2 ($\rho_{Z_{1Z_2}}$) for domes with different height-to-span ratios, an increase in the positive/negative correlation coefficient increases/decreases the reliability.

7- 6- Comparison of the effects of rigid and hinged nodes on the reliability

Modeling members' connections (joints) is an important task in the design of single-layered space domes. Although they are usually modeled rigidly (fixed) to prevent structure instability, most recent papers have considered them to be hinged. The current study has examined the effects of both rigid and hinged joints on the reliability of space domes with different height-to-span ratios (Fig. 9).

Internal forces are mainly flexural, and the related effects are negligible, but they cause errors in reliability calculations. However, an increase in the height-to-span ratio will increase the dome curvature causing its arch behavior to reduce the bending moment and increase the axial force in the members. At height-to-span ratios > 0.3, the members' bending moments reduce considerably due to which the difference between the reliabilities found by rigid and hinged joints is small.

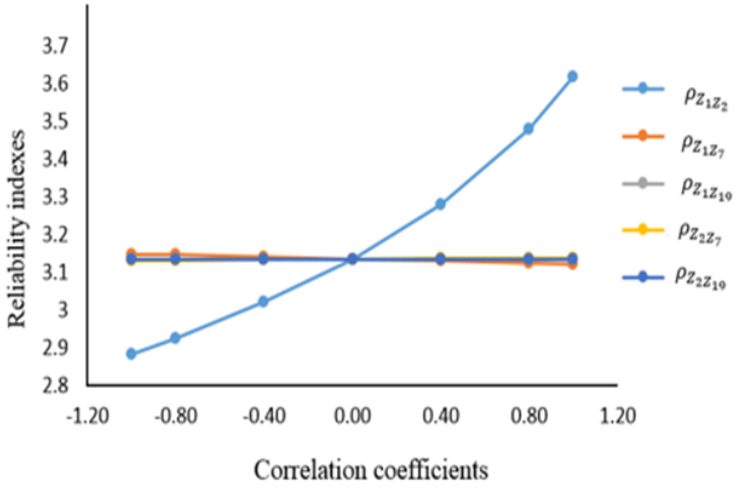

Fig. 7. Effects of inter-node correlation coefficient on the reliability index.

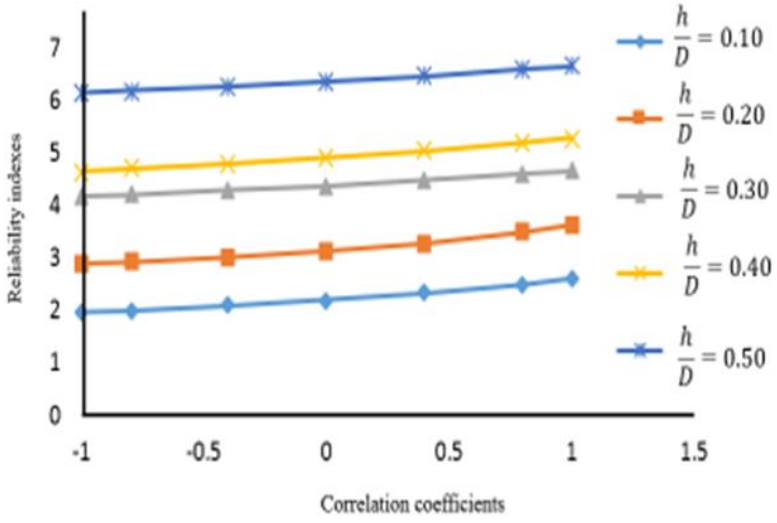

Fig. 8. Effects of inter-z1-z2-node correlation coefficient variations on the reliability index in domes with different height-to-span ratios.

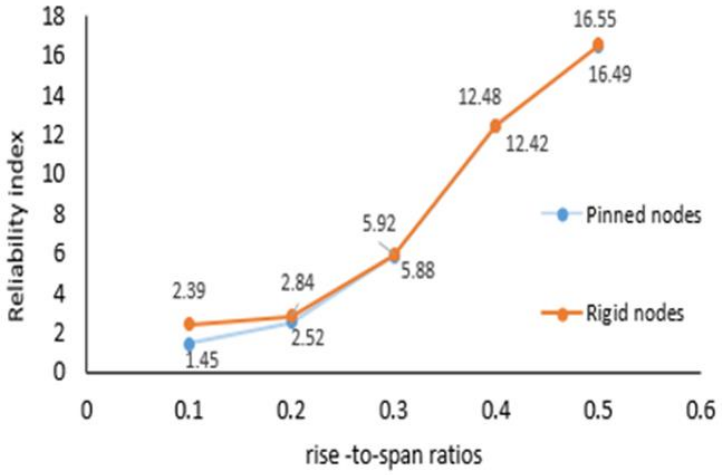

Fig. 9. Comparison of the reliability index of space domes with rigid and hinged nodes.

8- Conclusion

This paper has studied the effects of space domes' different height-to-span ratios on the reliability, sensitivity, and correlation among random variables and concluded the following:

1- Reliability indices of space domes with different height-to-span ratios were calculated by FORM, SORM, IS, and MCS, and the results showed that in domes with numerous random variables, the first two performed faster than MCS and IS, and their reliability indices were close, concluding that FORM could be used to continue the work.

2- In space domes with a ratio of height to opening less than 0.3, the effective function is the displacement function, and for ratios greater than 0.3, the stress function should be considered as the critical function.

3- For the displacement performance function, an increase in the height-to-span ratio did not change the sensitivity to the random variations of the space dome's nodes' coordinates.

4- An increase in the height-to-span ratio gradually increased the coefficients of the sensitivity of the displacement and stress performance functions to the changes in the external loads. Since an increase in the height-to-span ratio reduced the maximum deformation.

5- The change in the correlation coefficient between the members' elasticity moduli and the yield stress random variable (ρ_{EF_y}) at the height-to-span ratio of 0.1 and 0.2 changed the reliability, but in other ratios, the change in the correlation coefficient did not increase or decrease the reliability.

References

[1] Technology Performance Adjutancy, Design of Space Frame Structures Code, Publication 400, President Planning Adjutancy, 2004.

[2] H. Nooshin, Formex configuration processing in structural engineering, Elsevier Applied Science Publishers Ltd, Ripple Rd, Barking, Essex, U. K, 1984. 273, (1984).

[3] G. Parke, P. Disney, Space structures 5, Thomas Telford, 2002.

[4] I. Arjamandi, modern building skeletons, Tehran University Press 1996.

[5] L. Hui-Jun, P. Zeng-Li, Y. Chun-Liang, T. Yue-Ming, Application of advanced reliability algorithms in truss structures, International Journal of Space Structures, 29(2) (2014) 61-70.

[6] M.R. Sheidaii, Evaluation of probabilistic effect on the reliability of the network layer imperfection Space, Civil and Environmental Magazine, 40 (2010).

[7] L. Hui-Jun, W. Zheng-Zhong, L. Zhan-Chao, Reliability and sensitivity analysis of dendriform structure, International Journal of Space Structures, 28(2) (2013) 75-86.

[8] K. Kubicka, U. Radoń, W. Szaniec, U. Pawlak, Comparative analysis of the reliability of steel structure with pinned and rigid nodes subjected to fire, in: IOP Conference Series: Materials Science and Engineering, IOP Publishing, 2017, pp. 022051.

[9] M.T. Roudsari, M. Gordini, Random imperfection effect on reliability of space structures with different supports, Structural Engineering and Mechanics, 55(3) (2015) 461-472.

[10] L. Hui-Jun, L. Chun-Guang, J. Ling-Ling, Reliability and sensitivity analysis of double-layer spherical latticed shell, International Journal of Space Structures, 26(1) (2011) 19-29.

[11] H.-J. Li, C.-G. Liu, F. Jiao, G.-F. Lin, Reliability and sensitivity evaluation of nonlinear space steel structures, Journal of the International Association for Shell and Spatial Structures, 52(2) (2011) 97-107.

[12] C.K. Soh, J. Yang, Fuzzy controlled genetic algorithm search for shape optimization, Journal of computing in civil engineering, 10(2) (1996) 143-150.

[13] J. Salajegheh, M. Khatibinia, M. Mashayekhi, Optimization of the shape of a single-layer space dome using Binary Algorithm, in: Fourth National Congress of Civil Engineering, University of Tehran, 2009.

[14] M. Saka, Optimum topological design of geometrically nonlinear single layer latticed domes using coupled genetic algorithm, Computers & structures, 85(21-22) (2007) 1635-1646.

[15] O. Hasançebi, F. Erdal, M.P. Saka, Optimum design of geodesic steel domes under code provisions using metaheuristic techniques, International Journal of Engineering and Applied Sciences, 2(2) (2010) 88-103.

[16] S.-b. Qi, G.-y. Huang, X.-d. Zhi, F. Fan, Sensitivity analysis and probability modeling of the structural response of a single-layer reticulated dome subjected to an external blast loading, Defense Technology, (2022).

[17] G. Zhou, Q. Song, A. Li, S. Shen, Q. Zhou, B. Wang, Assessment on the Progressive Collapse Resistance of a Long-Span Curved Spatial Grid Structure With Main Trusses, KSCE Journal of Civil Engineering, 26(3) (2022) 1239-1253.

[18] H. Jahangir, M. Bagheri, S.M.J. Delavari, Cyclic behavior assessment of steel bar hysteretic dampers using multiple nonlinear regression approach, Iranian Journal of Science and Technology, Transactions of Civil Engineering, 45(2) (2021) 1227-1251.

[19] V. Farhangi, H. Jahangir, D.R. Eidgahee, A. Karimipour, S.A.N. Javan, H. Hasani, N. Fasihihour, M. Karakouzian, Behaviour investigation of SMA-equipped bar hysteretic dampers using machine learning techniques, Applied Sciences, 11(21) (2021) 10057.

[20] D. Pakseresht, S. Gholizadeh, Metaheuristic-based sizing and topology optimization and reliability assessment of single-layer lattice domes, Iran University of Science & Technology, 11(1) (2021) 1-14.

[21] L.-m. Tian, J.-p. Wei, Q.-x. Huang, J.W. Ju, Collapse-resistant performance of long-span single-layer spatial grid structures subjected to equivalent sudden joint loads, Journal of Structural Engineering, 147(1) (2021) 04020309.

[22] M. Zhang, X. Gao, X. Xie, A. Behnejad, G. Parke, A method to directly estimate the dynamic failure peak ground acceleration of a single-layer reticulated dome, Thin-Walled Structures, 175 (2022) 109188.

[23] A.S. Nowak, Collins, K.R., Reliability of Structures, McGraw-Hill, New York, 2000.

[24] Iranian Code of Practice for Seismic Resistant Design of Building, BHRC Publication, Tehran, 2006. (In Persian).

[25] A. Construction, Manual of steel construction: allowable stress design, American Institute of Steel Construction: Chicago, IL, USA, (1989).

[26] J.D. Sørensen, Notes in structural reliability theory and risk analysis, Aalborg University, 4 (2004).

[27] M.R. Rajashekhar, B.R. Ellingwood, A new look at the response surface approach for reliability analysis, Structural safety, 12(3) (1993) 205-220.

[28] S. Rahman, D. Wei, A univariate approximation at most probable point for higher-order reliability analysis, International journal of solids and structures, 43(9) (2006) 2820-2839.

[29] S.-K. Choi, R.A. Canfield, R.V. Grandhi, Reliability-Based Structural Optimization, Springer, 2007.

[30] Q. Chen, Reliability-based structural design: a case of aircraft floor grid layout optimization, Georgia Institute of Technology, 2011.

[31] M. Gordini, M. Habibi, M. Tavana, M. TahamouliRoudsari, M. Amiri, Reliability analysis of space structures using Monte-Carlo simulation method, in: Structures, Elsevier, 2018, pp. 209-219.

[32] M.A. Shayanfar, M.A. Barkhordari, M.A. Roudak, An efficient reliability algorithm for locating design point using the combination of importance sampling concepts and response surface method, Communications in Nonlinear Science and Numerical Simulation, 47 (2017) 223-237.

[33] H.O. Madsen, S. Krenk, N.C. Lind, Methods of structural safety, Courier Corporation, 2006.

[34] I. Kaymaz, Approximation methods for reliability-based design optimization problems, GAMM-Mitteilungen, 30(2) (2007) 255-268.

[35] R. Rackwitz, B. Flessler, Structural reliability under combined random load sequences, Computers & structures, 9(5) (1978) 489-494.

[36] P. Liu, Der Kiureghian: A. Optimization algorithms for structural reliability, Structural Safety, 9(3) (1991) 161-177.

[37] K. Breitung, Asymptotic approximations for multinormal integrals, Journal of Engineering Mechanics, 110(3) (1984) 357-366.

HOW TO CITE THIS ARTICLE

A. Bahrpeymah, M. Layegh Rafat, N. Shabakhty, Reliability of Single-Layer Steel Space Domes under the Effects of the Changes in the Height-to-Span Ratio, AUT J. Civil Eng., 6(1) (2022) 3-14.

DOI: 10.22060/ajce.2022.19547.5740